

# BENDING DEFLECTIONS DUE TO SCRIBE-INDUCED RESIDUAL STRESSES

B. Austin, B. Love, T. Dow, J. Eischen and R. Scattergood  
Precision Engineering Center, NCSU, Raleigh, NC 27695-7918

## Introduction

When a sharp diamond tip is translated across the surface of a specimen, a scribe trace will be generated. This is a source of residual stress. The stress is due to the elastic-plastic constraint associated with the deformed material that is displaced from the trace. When scribes are made across a plate sample, the residual stresses will cause bending distortions orthogonal to the scribe trace. This effect can be used to produce nanometer-scale shape changes that can be useful in manufacturing applications such as disk read-write heads [1]. The objective of the work reported here was to produce a model for the bending effect. The model uses the elastic stresses caused by a line-force dipole to approximate the scribe-induced residual stresses. Scribing experiments were made to verify the accuracy of the model.

## Model

Consider a line-force dipole acting on the surface of an elastic half-space shown in Figure 1. The force dipole lies along the  $z$ -axis.  $F$  is the line force per unit length,  $a$  is the force spacing and  $B = Fa$  is the dipole strength. A force-dipole model consisting of two orthogonal pairs of discrete dipole forces acting on the surface of an elastic half space was introduced by Yoffe [2] as a model for the residual stresses due to a single indentation. The scribe can be viewed as the superposition of a series of indentations that produce a line-force dipole [3]. The stresses due to a line-force dipole acting on an elastic half space can be evaluated using the equations given by Johnson [4].

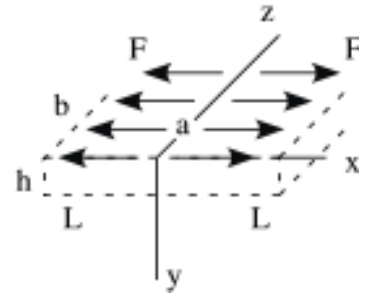


Fig. 1. Line-Force dipole

For the analysis of the bending effect, consider a finite rectangular plate with a central scribe along the  $z$ -axis in Figure 1. The finite-body stress solution requires that the stress field due to the half-space line-force dipole vanish on the plate surfaces. If the plate thickness  $h$  is small compared to its length  $2L$  and width  $b$ , the magnitude of the stress acting on the plate edges is negligible. However, the normal and shear stresses,  $\sigma_{yy}$  and  $\sigma_{xy}$ , which act on the bottom surface cannot be ignored. The equilibrium configuration (bending effect) is obtained by applying the reversed dipole stresses to the bottom surface of the plate and then solving a beam-bending problem with these stresses as the loading functions [5]. This is not an exact solution for the internal stresses, however, the relevant force and moment equilibrium conditions are satisfied. FEM calculations showed that the shape profile errors are negligible using this approximation. Equation (1) is the solution of the beam-bending problem for the bend angle,  $\phi(X)$ , and the displacement,  $\delta(X)$ . The normalized distance along the plate is  $X = x/h$ ,  $B$  is the dipole strength (taken in the limit  $F \rightarrow \infty$  and  $a \rightarrow 0$  such that  $B$  is fixed),  $E$  is the elastic modulus and  $h$  is the

thickness. After shifting the functions given in equation (1) by multiples of the scribe spacing, superposition can be used to obtain the equivalent results for multiple scribes.

$$\begin{aligned}\phi(X) &= -\frac{6B}{\pi E h^2} \left[ \tan^{-1}(X) + \frac{X}{1+X^2} \right] = \frac{6B}{\pi E h^2} f(X) \\ \delta(X) &= -\frac{6B}{\pi E h} \left[ X \tan^{-1}(X) \right] = \frac{6B}{\pi E h} g(X)\end{aligned}\quad (1)$$

Figure 2 shows the form of the functions  $f(X)$  and  $g(X)$  defined in equation (1) for a single central scribe (only half of the symmetric profile is shown). By definition,  $\phi(X)$  and  $\delta(X)$  are the tangent angle and the displacement at  $X$  measured downward (negative) from the  $x$ -axis, hence,  $g(X)$  is equivalent to the profile shape. The bend-angle function  $f(X)$  approaches  $-\pi/2$  as  $X$  increases and the displacement function  $g(X)$  becomes linear. Therefore, the bending effect appears as a localized “hinge” around the scribe trace at  $X = 0$ . Similar features are obtained for multiple scribes symmetrically placed around a central scribe. In order to compare the predictions of the model to actual profiles, the dipole strength  $B$  in equation (1) must be evaluated. For a given scribe tip geometry and material, the normal load applied to the scribe is the dominant parameter determining the residual stresses and the dipole strength. In order to calibrate the model for verification purposes, the procedure adopted here was to measure the average bend angle as a function of the scribe load  $W$ . By equating  $\phi(X)$  in equation (1) to the measured angles, a relation between  $B$  and  $W$  can be obtained. This will be the calibration curve for the given scribing geometry and material parameters.

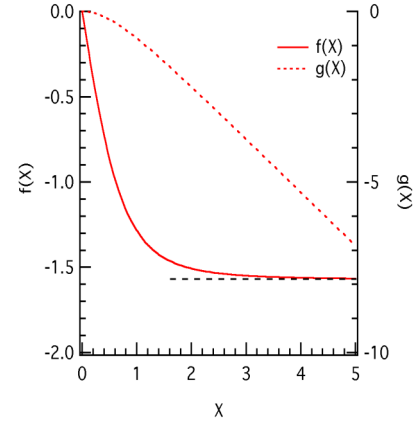


**Fig. 2.**  $f(X)$  and  $g(X)$  functions.

### Scribing Tests and Model Verification

The scribing tests were done using Dynatex V4-64 diamond scribing tips, with the scribe axis tilted  $32^\circ$  from vertical, and the modified Zwick hardness tester shown in Figure 3. The samples were translated in the scribing direction using a motorized  $x$ - $y$  stage. The test material was  $Al_2O_3$ -TiC (30 volume % TiC) and for most of the tests the samples were ceramic plates measuring approximately 1 mm x 1 mm x 0.3 mm thick. Displacement profiles were measured using a New View optical profilometer. The difference between the initial sample profile and the profile after scribing, adjusted for tilt, produced the bend profile for the given scribing conditions. A series of tests were made using scribing loads in the range  $0.031 \text{ N} \leq W \leq 1.71 \text{ N}$  to establish the bend angle vs. scribe load relationship. This data was used to establish the dipole



**Fig. 3.** Setup for scribing tests.

strength vs. scribe load relationship shown in Figure 4 ie., the  $B$  vs.  $W$  calibration curve [5]. Verification of the model was based on a comparison of the measured displacement profiles with the model prediction for  $\delta(X)$  given in equation (1) using the  $B$  values from Figure 4. This comparison is considered to be a primary benchmark since the displacements are usually the quantities of interest for applications [1]. Figures 5a and 5b show typical examples of the measured displacement profiles (solid) and the model predictions (dashed) for test samples used to generate the calibration curve in Figure 4. The spikes on the measured curves are profilometer dropouts that correspond to the positions of the three scribes made per test sample. The agreement is very good over the range of the loads used. Figure 6 shows an example of the measured displacement profile (solid) and the model prediction (dashed) for a sample tested under different conditions (5 mm sample length and five scribes). The agreement is again very good which verifies the fact that the calibration curve shown in Figure 4 is a master curve for the given scribing conditions and material properties.

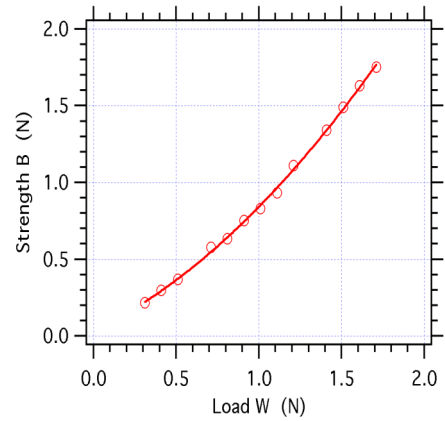


**Fig. 4.**  $B$  vs  $W$  calibration curve.

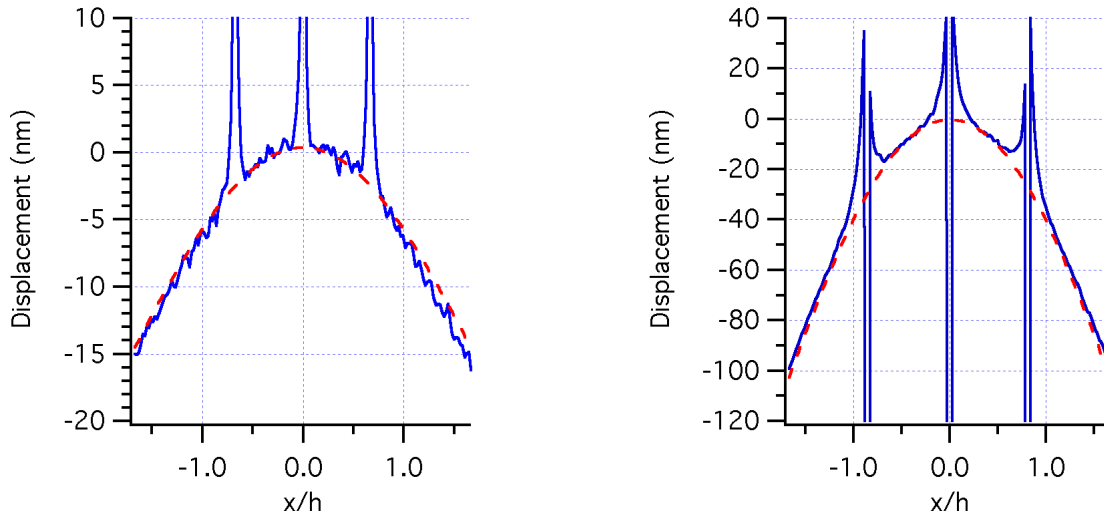


**Fig. 5.** a)  $W = 0.31$  N,  $B = 0.22$  N.

b)  $W = 1.61$  N,  $B = 1.75$  N.

For the model calculations and the verification results shown in Figures 5 and 6, scribes were made across the entire width of a plate sample. This is essentially a 1D problem, which is suitable for calibration and verification of the force-dipole model based on Figure 1 and equation (1). However, in practical applications where scribing is used to either produce a certain shape on a component or correct a form error [1], scribes of various lengths and orientations will be required. This becomes a 2D problem that is more difficult to solve and, in general, is not amenable to simple analytical results of the kind obtained in equation (1). The approach in this case requires the use of FEM to obtain solutions for displacement profiles due to partial scribes

(line-force dipoles) on the surface of plate samples. For given scribing conditions, calibration data like that shown in Figure 4 can be used to obtain the dipole strengths required as input for the FEM calculations. Studies are currently underway to implement and verify an FEM-based 2D model using line-force dipoles [6]. Figure 7 shows a typical FEM result for a partial scribe made across a plate sample. In this case there are curvatures around two principal axes.

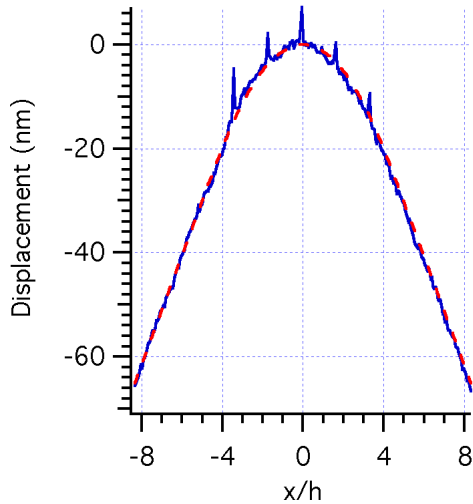


**Fig. 6.**  $W = 0.16$  N,  $B = 0.0864$  N. Five scribes indicated by the peaks were made on a 1 mm x 5 mm x 0.3 mm  $\text{Al}_2\text{O}_3$ -TiC sample.

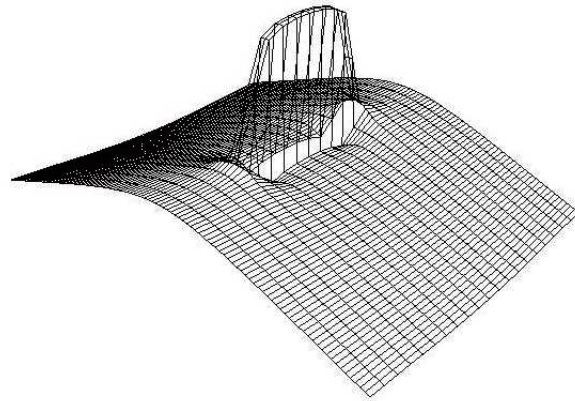


**Fig. 7.** FEM calculation for the displacement profile due to a partial scribe. The discrete peak is an artifact showing the scribe location.

## Conclusions

The comparisons of the measured and model displacement profiles presented in Figures 5 and 6 show that the line-force dipole model provides a very good representation of scribe-induced residual stresses and the associated bending effects. Processes that produce similar types of residual stress, for example, grinding or laser-melt scribing, may also be amenable to force-dipole models provided that the models are suitably modified to account for the differences in the elastic-plastic constraints.

## References

1. A. C. Tam, C. C. Poon, L. Crawforth and P. M. Lundquist, "Stress on the Dotted Line", *Data Storage*, vol. 6, issue 13, 29 (1999).
2. E. H. Yoffe, "Elastic Stress Fields Caused by Indenting Brittle Materials", *Phil. Mag. A*, vol. 46, no. 4, 617 (1982).
3. Y. Ahn, T. N. Farris and S. Chandraskar, "Elastic Stress Fields Caused by Sliding Microindentation of Brittle Materials", *Proc. of the Int. Conf. On Machining of Advanced Materials*, S. Jahanimir, ed., NIST Spec. Publ. 847, 71 (1993).
4. K. L. Johnson, "Contact Mechanics", Cambridge Univ. Press, p.17 (1985).
5. B. Austin, MS Thesis, North Carolina State University (2000).
6. B. Love, MS Thesis, North Carolina State University (in progress).